28 GHz Bandpass Filter using Liquid Crystal Polymer (LCP)

Yuta Hasegawa,[1] Masayuki Ota,[2] Toshiya Iwamura,[3] Yusuke Nakatani,[2] and Naoki Oyaizu[1]

We present three types of bandpass filters operating at 28 GHz with 5th-order Chebyshev, 4th-order canonical and 6th-order canonical stages. All of them are made of liquid crystal polymer (LCP) with solder bump input and output transition to printed circuit board (PCB) and are optimized to have very compact size. First, the characteristics of the filters are estimated by the coupling matrix. Then they are designed by electromagnetic simulation and are fabricated by PCB process. Measurement demonstrates that peak of |S21| is 3.1 dB for the fifth-order Chebyshev, 2.2 dB for the fourth-order canonical, and 2.8 dB for the sixth-order canonical filters. 1-dB bandwidth is 2.9 GHz for the fifth-order Chebyshev, 2.45 GHz for the fourth-order canonical and 2.45 GHz for the sixth-order canonical. 25-dB bandwidth is 5.52 GHz for the fifth-order Chebyshev, 5.79 GHz for the fourth-order canonical, and 4.61 GHz for the sixth-order canonical.

1. Introduction

Millimeter-wave antennas used in 5G systems have large radiation gain because electricity is fed to their many antenna elements and enhance the directivity. Therefore, a band-pass filter with sharp roll-off characteristics is required to suppress radiation (spurious signals) outside a specified frequency band. Furthermore, since components such as a radio frequency integrated circuit (RFIC), a bandpass filter (BPF), and a combiner are mounted on the antenna board, each component needs to be small [1]. In millimeter-wave-band systems, waveguide-type and strip-line-type filters are mainly used. Waveguide-type filters have a high unloaded Q factor, which affects the characteristics of the filters. This allows low insertion loss and sharp roll-off, but requires that the size of the resonator be about a half wavelength square. Although strip-line-type filters require a half wavelength for the line, the filters can be made smaller because they can be bent. However, because the filters suffer greater loss due to the small unloaded Q factor, the development of a sharp roll-off filter is difficult [2].

To develop a small, sharp roll-off filter, filters with cross-coupling were used for testing. First, coupling matrix is derived in order to consider the filters with cross-coupling. Next, after the changes in the characteristics of filters by the coupling topology at each unloaded Q factor were compared using the coupling matrix, they were designed by electromagnetic field simulation. We fabricated the filters by a general printed circuit board (PCB) process and attached each filter to a PCB by solder bumps.

1 : Electronic Technologies R&D Center
2 : Print Circuit Board Division
3 : Tohoku Fujikura Ltd.

2. Coupling Matrix

In millimeter-wave band systems, resonator-coupled BPFs are mainly used. The S parameter of a resonator-coupled BPF is obtained using the coupling matrix, which shows the coupling topology. First, the circuit equation of the resonator-coupled filter is obtained from Kirchhoff's law, and the coupling matrix is deduced[3].

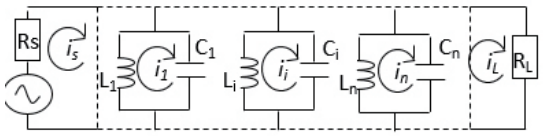

Fig. 1. Circuit of filter.

Consider a filter in which n resonators are coupled as shown in Fig. 1. Let i_i be the current flowing through the i-th closed loop, L_i be the inductance, C_i be the capacitance, R_s be the power supply resistance, R_L be the load resistance, and L_{ij} be the mutual inductance between the resonators, and the following equation is obtained:

$$\begin{bmatrix} R_s & -j\omega L_{s1} & \dots & -j\omega L_{1n} & -j\omega L_{sL} \\ -j\omega L_{1s} & j\omega L_1 + \frac{1}{j\omega C_1} & \dots & -j\omega L_{1n} & -j\omega L_{1L} \\ \dots & \dots & \dots & \dots & \dots \\ -j\omega L_{ns} & -j\omega L_{n1} & \dots & j\omega L_n + \frac{1}{j\omega C_n} & -j\omega L_{nL} \\ -j\omega L_{Ls} & -j\omega L_{L1} & \dots & -j\omega L_{Ln} & R_L \end{bmatrix} \begin{bmatrix} i_s \\ i_1 \\ \dots \\ i_n \\ i_L \end{bmatrix} = \begin{bmatrix} e_s \\ 0 \\ \dots \\ 0 \\ 0 \end{bmatrix}$$

This expresses the impedance matrix $[Z]$ × current vector $[i]$ = voltage vector $[e]$.

Here, L and C of each resonator are assumed to be equal. We also have fractional bandwidth (FBW) of.

$$p = \frac{1}{FBW}\left(\frac{\omega}{\omega_0} - \frac{\omega_0}{\omega}\right)$$

to perform the frequency conversion of a low-pass filter and a band-pass filter.
For each of the bonds

$$M_{ij} = \frac{L_{ij}}{L}$$

$$\text{and, } \frac{\omega}{\omega_0} \fallingdotseq 1$$

$$m_{ij} = \frac{M_{ij}}{FBW}$$

$$\frac{R_i}{\omega_0 L \cdot FBW} = R_{0i} \qquad i = S, L$$

using $[Z] = \omega_0 L \cdot FBW[\bar{Z}]$ can be expressed as

$$[\bar{Z}] = \begin{bmatrix} R_{0s} & -jM_{s1} & \cdots & -jM_{sn} & -jM_{sL} \\ -jM_{1S} & jp - jM_{11} & \cdots & -jM_{1n} & -jM_{1L} \\ \cdots & \cdots & \cdots & \cdots & \cdots \\ -jM_{nS} & -jM_{n1} & \cdots & jp - jM_{nn} & -jM_{nL} \\ -jM_{LS} & -jM_{L1} & \cdots & -jM_{Ln} & R_{0L} \end{bmatrix}$$

When $[R]$ = diag $[R_{0S}, 0, ..., 0, R_{0L}]$, $[U]$ = diag [0,1, ..., 1,0], $[M]$ which appears by decomposing $[\bar{Z}] = [R] + jp[U] + j[M]$ is the connex matrix. The diagonal component of $[M]$ represents the resonance frequency, and the others represent the coupling between resonators. Given the coupling topology of the filter, we can know $[M]$ and obtain $[Z]$.

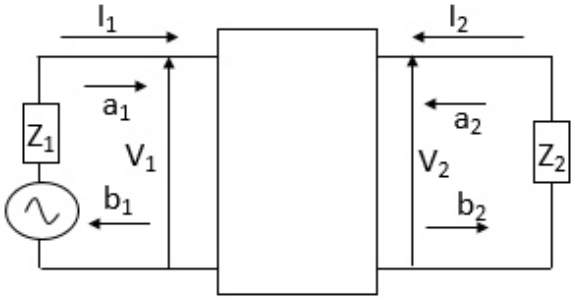

Fig.2. Circuit of 4 ports.

Then S11 and S21 are obtained from $[Z]$. Consider the S-parameter of a two-terminal pair circuit as shown in Figure 2. If ai is the incidental wave and b_i is the reflected wave,

$$a_i = \frac{V_i + Z_i I_i}{2\sqrt{Z_i}}$$

$$b_i = \frac{V_i - Z_i I_i}{2\sqrt{Z_i}}$$

are defined. Since $I_1 = i_s$, $V_1 = e_s - i_s R_s$ $I_2 = -i_L$ from Figure 1

$$a_1 = \frac{e_s}{2\sqrt{R_s}}$$

$$b_1 = \frac{e_s - 2i_s R_s}{2\sqrt{R_s}}$$

$$a_2 = 0$$

$$b_2 = i_L\sqrt{R_L}$$

and thus,

$$S_{11} = \frac{b_1}{a_1} = 1 - \frac{2R_s i_s}{e_s} = 1 - 2R_s[Z]^{-1}_{1,1}$$

$$S_{21} = \frac{b_2}{a_1} = \frac{2i_L\sqrt{R_s R_L}}{e_s} = 2\sqrt{R_s R_L}[Z]^{-1}_{n+2,n+2}$$

can be calculated.

3. Influence of coupling topology

When a strip-line-type resonator is used, the unloaded Q factor is generally about 30 - 200. Taking this into consideration, the unloaded Q factor was set at 30 - 200 to examine the effect on the transmission characteristics. Using the coupling matrix, the following three types of filters were examined: fifth-order Chebyshev-type filter which is expected to suppress spurious noise outside the band and has sharp roll-off characteristics to some extent, fourth- and sixth-order canonical-type filters which have sharp roll-off characteristics because they have transmission zero points outside the passband.

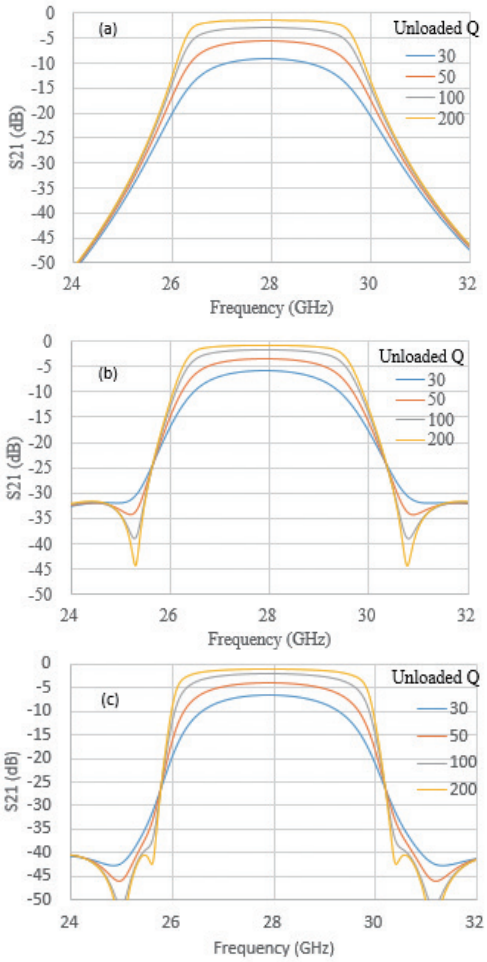

Fig.3. S21 as changing unloaded Q factor (a) 5th order chebyshev (b) 4th order canonical (c) 6th order canonical.

The FBW was determined so that the 1-dB band becomes 2.5 GHz when the unloaded Q factor is 100, and then the factor was changed for comparison. Figure 3 shows that loss increases as the unloaded Q factor decreases, and the

curve becomes smoother.

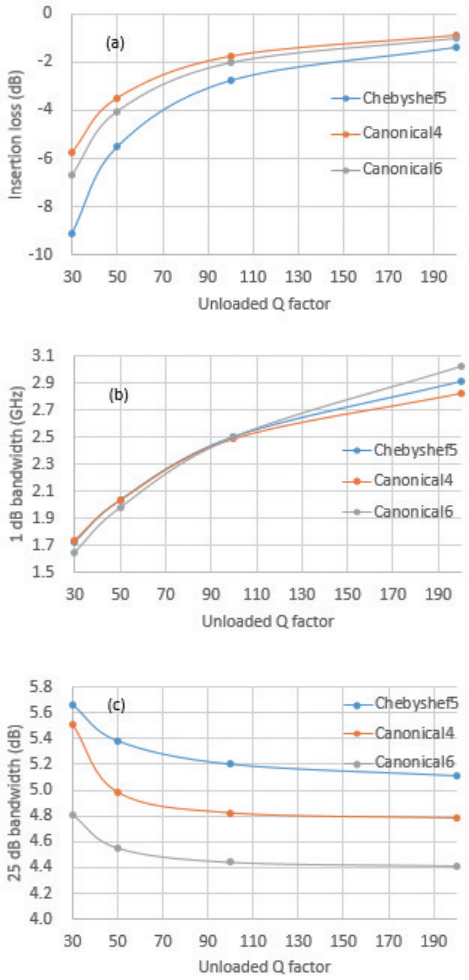

Fig.4. Unloaded Q factor dependence of (a) peak of passband, (b) 1 dB bandwidth, (c) -25 dB bandwidth.

Figure 4 shows three graphs of insertion loss (a), 1-dB bandwidth (b), and 25-dB bandwidth (c) when unloaded Q factor is changed. In the low unloaded Q region, the 1 dB bandwidth is less affected by the coupling topology, but the insertion loss and the 25-dB bandwidth are affected by the coupling topology.

4. Design of Filter

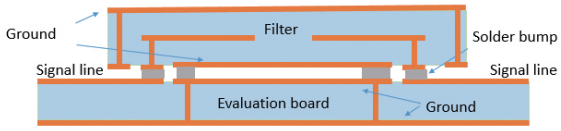

Fig.5. Side view of filter

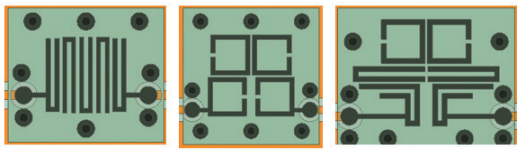

Fig.6. Over view of filter (L) 5th order series (C) 4th order canonical (R) 6th order canonical

Figure 5 shows a cross-sectional view of structures that we used for simulation, and Fig. 6 shows top views of the structures. These filters use a liquid crystal polymer (LCP) substrate consisting of three conductor layers. The thickness of each LCP between conductors is about 100 μm. The first conductor layer from the top consists of a ground, the second layer signal lines includes a resonator, and the third layer a ground and an input/output port. The ground of the first layer and the ground of the third layer are connected by vias, and the signal line of the second layer and the input/output port of the third layer are also connected by vias. The input/output port and the ground of the third layer are connected to each signal line and ground on the evaluation substrate by solder bumps.

The coupling topology of each filter is obtained by a wiring pattern as shown in Fig. 6. In the fifth-order series bandpass filter, five U-shaped resonators are alternately arranged, and each resonator is magnetically coupled. The fourth-order canonical bandpass filter consists of four C-shaped resonators. The first and fourth stages are arranged so as to face each other and form electric field coupling, and the first and second stages, the second and third stages, and the third and fourth stages are arranged so as not to face each other and form magnetic field coupling. However, because unexpected coupling occurs in stages 1 and 3, and 2 and 4, the out-of-band transmission zero point shifts to the low frequency side. To reduce the power level to about 30 dB at the high frequency side, the coupling between the first and fourth stages is weakened more than expected, and the transmission zero point is separated from the center. Therefore, the roll-off characteristics are milder than those calculated by the coupling matrix. The sixth-order canonical filter consists of six resonators. Each of the first and the sixth are an L-shape, the second and the fifth a U-shape, and the third and the fourth a C-shape.

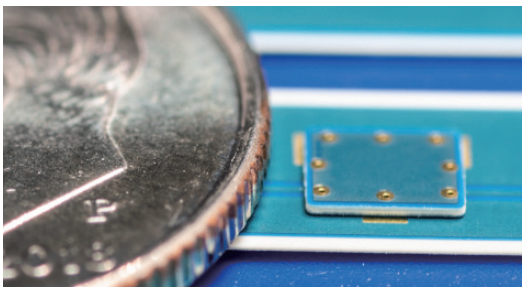

Fig.7. Picture of filter

Figure 7 shows the simulation results. The peak of |S21| is 3.3 dB for the fifth-order Chebyshev, 2.3 dB for the fourth-order canonical, and 2.8 dB for the sixth-order canonical filters. The 1-dB bandwidth is 2.6 GHz for the fifth-order Chebyshev, 2.9 GHz for the fourth-order canonical and 2.6 GHz for the sixth-order canonical, the 25-dB bandwidth is 5.7 GHz for the fifth-order Chebyshev, 6.1 GHz for the fourth-order canonical, and 4.9 GHz for the sixth-order canonical,. The fourth-order canonical filter has the lowest insertion loss and the sixth-order canonical filter has the steepest roll off while the insertion loss is lower than 3 dB.

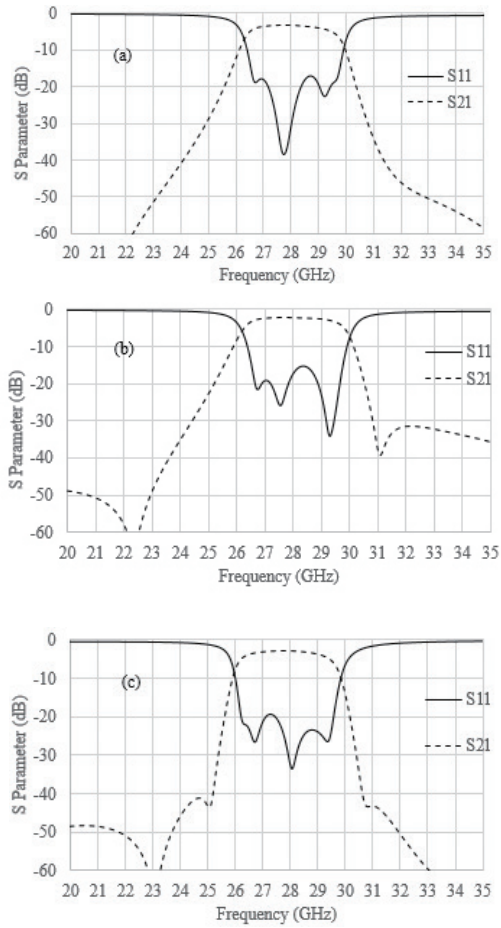

Fig.8. Simulation results (a) 5th order series (b) 4th order canonical (c) 6th order canonical.

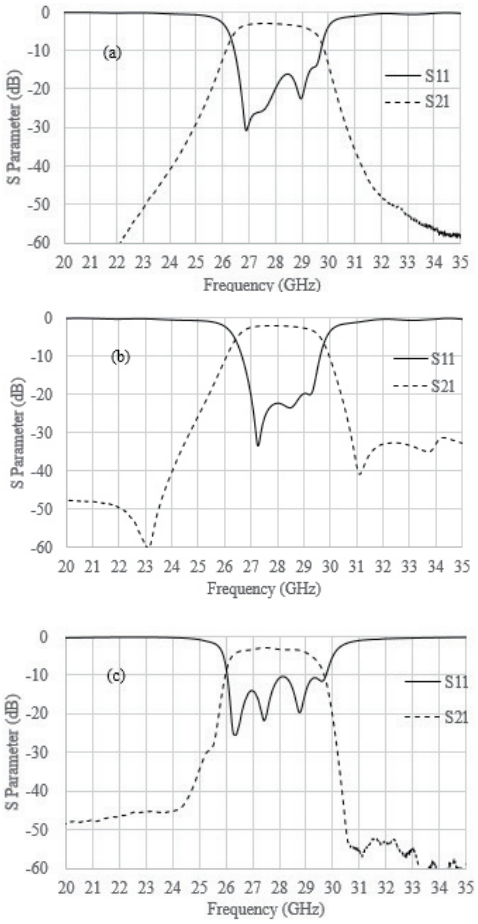

Fig.9. Measurement results (a) 5th order series (b) 4th order canonical (c) 6th order canonical.

5. Measurement

Figure 8 is a photograph of the fabricated filter. The probe was applied to the probe pad on the evaluation substrate, and measurements were carried out. The fabricated filter was connected to the evaluation substrate through the solder bump. The thickness of the filter is 330 μm including the solder resist layer covering the upper and lower layers.

The measured results are shown in Fig. 9. Peak of |S21| is 3.1 dB for the fifth-order Chebyshev, 2.2 dB for the fourth-order canonical, and 2.8 dB for the sixth-order canonical filters. 1-dB bandwidth is 2.9 GHz for the fifth-order Chebyshev, 2.45 GHz for the fourth-order canonical and 2.45 GHz for the sixth-order canonical, 25-dB bandwidth is 5.52 GHz for the fifth-order Chebyshev, 5.79 GHz for the fourth-order canonical, and 4.61 GHz for the sixth-order canonical.

6. Conclusion

Three kinds of 28 GHz band bandpass filters were fabricated using LCP substrate, and their characteristics were measured. The filters with cross coupling have lower loss and higher selectivity than conventional series (Chebyshev) ones. Especially, the sixth-order canonical filter can reduce LO signals by more than 35 dB. All of them are smaller than 4×4×0.4 mm^3 and attached to PCB by solder bumps. The manufacturability and compactness as well as high performance of these filters make them promising solutions for 5G mmWave applications.

Reference

1) B. Sadhu, Y. Tousi, J. Hallin, S. Sahl, S. K. Reynolds, Ö. Renström, K. Sjögren, O. Haapalahti, N. Mazor, B. Bokinge, G. Weibull, H. Bengtsson, A. Carlinger, E. Westesson, J-E. Thillberg, L. Rexberg, M. Yeck, X. Gu, M. Ferriss, D. Liu, D. Friedman, and A. Valdes-Garcia, "A 28-GHz 32-element TRX phased-array IC with concurrent dual-polarized operation and orthogonal phase and gain control for 5G communications," IEEE Trans. Solid-State Circuits, vol. 52, no. 12, pp. 3373-3391, Dec. 2017.
2) X. Chen and K. Wu, "Substrate integrated waveguide filter: basic design rules and fundamental structure features," IEEE Microwave Magazine, vol. 15, no. 5, pp. 108-116, July-Aug. 2014.
3) J-S. Hong, "Microstrip Filters for RF/Microwave Applications," Second Ed., Wiley, 2011.